PERGAMON

International Journal of Solids and Structures 37 (2000) 5315–5327

INTERNATIONAL JOURNAL OF SOLIDS and STRUCTURES

www.elsevier.com/locate/ijsolstr

# Fracture toughening mechanism of shape memory alloys due to martensite transformation

Sung Yi*, Shan Gao

*School of Mechanical and Production Engineering, Nanyang Technological University, Nanyang Avenue, North Spine (N3), Level 2, Singapore 639798, Singapore*

Received 23 March 1999; in revised form 4 August 1999

**Abstract**

The fracture toughening mechanism of shape memory alloys is studied analytically. The asymptotic stress analysis of shape memory alloys under mode I loads is carried out using the Eshelby inclusion method and the weight function method. The toughening mechanism due to martensite transformation of shape memory alloys is investigated on the basis of the crack shielding theory of fracture mechanics. The transformation boundaries for static and steady advanced cracks are also determined. The analytic results show that the martensite transformation reduces the crack tip stress intensity factor and increases the toughness. The toughness of shape memory alloys is enhanced by the transformed strain fields which tend to limit or prevent crack opening and advancing. 

*Keywords:* Shape memory alloys; Fracture toughening mechanism

## 1. Introduction

In recent years, shape memory alloys (SMAs) have attracted the attention of scientific and engineering communities due to their potential use in many engineering applications (Birman, 1997; Chopra, 1996). SMAs are metal alloys that exhibit the special characteristics of either large recoverable strains or large induced internal forces under load and/or temperature changes. The unique thermo-mechanical properties of SMAs are due to a crystallographic phase transformation from the austenite/parent phase to the martensite/product phase or vice-versa. Martensite Transformations involve a lattice transformation featuring shear deformation and a coordinated atomic movement, which maintains the

* Corresponding author. Tel.: +65-790-6239; fax: +65-791-1859.
*E-mail address:* msyi@ntu.edu.sg (S. Yi).

0020-7683/00/$ - see front matter 
PII: S0020-7683(99)00213-9

one-to-one lattice correspondence between the lattice point in the parent and transformed phases (Funakubo, 1984). The martensitic phase is a substitutional or interstitial solid solution. The transformation is diffusion free which yields the same concentration of solute atoms dissolved in the martensitic phase as in the parent phase. Martensitic transformations are typically characterized by well-defined shape changes or surface relieves. Many researchers have studied the mechanical behavior of SMAs (Achenbach and Muller, 1983, 1986; Brinson and Lammering, 1993; Brinson and Huang, 1996; Tanaka, 1986, 1990; Sun and Hwang, 1993a, 1993b; Liang and Rogers, 1990, 1991). However, no work has been reported in the literature on the fracture toughness of SMAs due to martensite transformations.

The reduction of crack-tip stress intensity by the transformation-induced stresses is investigated in this paper. A fracture toughening mechanism is analyzed for particles which experience a deviatoric component of the macroscopic transformation strain. The transformation strain is then independent of the particle location within the crack-tip field. Therefore, the analysis is most pertinent to crack-tip transformations which induce an equal number of variants per particle. Transformations which produce a single variant per particle must also interact with the crack-tip shear strains to provide a further reduction in the stress intensity. In this study, the transformation-toughening behavior of SMAs under mode I loading is studied. For shape memory alloys, shear strains play an important role in the transformation process compared with previously studied materials such as zirconia ceramics (Budiansky et al., 1983; McMeeking and Evans, 1982; Evans, 1984; Stam and Giessen, 1995; Shen and Yu, 1996). Firstly, the shape and size of the transformation zone in both static cracked and steady advance cracked SMAs are described. Secondly, the effects of the transformation on the fracture toughness of shape memory alloys are investigated using Eshelby's inclusion method and the weight function method. The stress intensity factor due to the traction applied to the cylindrical particle is evaluated.

## 2. Analysis

### 2.1. Constitutive relations

There are two main approaches to establish constitutive relations of materials. One is the macroscopic phenomenological method that requires a significant amount of experimental work while the other is the microscopic physical method that derives the constitutive relation from fundamental physical concepts. The first attempts to mathematically describe a behavior of shape memory materials can be traced to the early work of Achenbach and Muller (1983, 1986). A macroscopic phenomenological model for shape memory alloys was proposed by Tanaka (1986, 1990) on the basis of the energy balance equation and the Clausius–Duhem inequality. Later it was modified by many other researchers (Brinson and Lammering, 1993; Brinson and Huang, 1996; Liang and Rogers, 1990, 1991). Boyd (1994) and Lagoudas et al. (1997) also proposed a constitutive model which accounts for simultaneous transformation and reorientation. Sun and Hwang (1993a, 1993b) presented a constitutive model which accounts for the effects of micro-structural physical mechanisms such as internal stress, twin boundary displacement and interface friction in the process of transformation or reorientation. It is possible to describe and interpret the various phenomena by using this unified inter-related model. Because no limitation is made to the loading history in derivation of this equation, the model is valid for the forward and reverse transformation processes under any non-proportional loading conditions and it can be concluded that the dependency on loading history is replaced by the current values of internal variables. In this study, Sun and Hwang's model is employed and the constitutive relations of shape memory alloys are

$$\dot{\epsilon}_{ij} = \dot{\epsilon}^{\mathrm{e}}_{ij} + \dot{\epsilon}^{\mathrm{p}}_{ij} = M_{ijkl}\dot{\sigma}_{kl} + \frac{\sqrt{3}g\left[S_{ij} - \xi B_1(T)\langle\epsilon^{\mathrm{p}}_{ij}\rangle\right]}{2J\left[S_{mn} - \xi B_1(T)\langle\epsilon^{\mathrm{p}}_{mn}\rangle\right]} \cdot \dot{\xi} \tag{1}$$

where

$$J\left[S_{mn} - \xi B_1(T)\langle\epsilon^{\mathrm{p}}_{mn}\rangle\right] = \left[\frac{3}{2}\left(S_{mn} - \xi B_1(T)\langle\epsilon^{\mathrm{p}}_{mn}\rangle\right)\left(S_{mn} - \xi B_1(T)\langle\epsilon^{\mathrm{p}}_{mn}\rangle\right)\right]^{1/2} \tag{2}$$

and

$$S_{ij} = \sigma_{ij} - \sigma_m\delta_{ij}$$

$$g = \sqrt{2}\left(\epsilon^{p}_{ij}\epsilon^{p}_{ij}\right)^{1/2}$$

$$\epsilon^{p}_{ij} = \frac{\sqrt{3}}{2}g\frac{S_{ij}}{\sigma_e} \tag{3}$$

In the above, the over dot represents the partial differentiation with respect to time, $\langle\ \rangle$ denotes average quantity, $\epsilon^{\mathrm{e}}_{ij}$ and $\epsilon^{\mathrm{p}}_{ij}$ are the elastic and plastic strains, respectively, $g$ is the intensity of $\epsilon^{\mathrm{p}}_{ij}$ associated with austenite-to-martensite transformation, $M_{ijkl}$ is the compliance of materials, $T$ is temperature, $\xi$ is the internal variant representing the transformed volume fraction of martensite, and $B_1(T)$, $C_0(T, \xi)$ are the material functions.

### 2.2. Stress field analysis

In this study, it is assumed that the height of the transformation zone is small compared with the length of a crack. Under this small scale transformation condition, an asymptotic problem can be formulated for a semi-infinite crack as shown in Fig. 1 where the stress field is given by

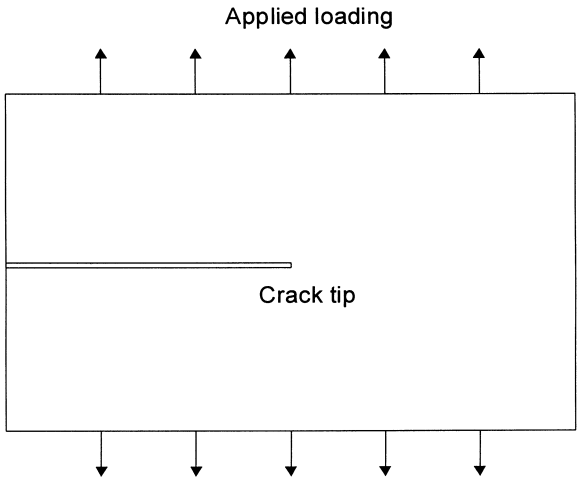


Fig. 1. A semi-infinite crack in homogeneous shape memory alloys.

$$\sigma_{ij} = \frac{K^{\infty}}{\sqrt{2\pi r}} \cdot f_{ij}(\theta) \tag{4}$$

where $K^{\infty}$ is the applied or remote stress intensity factor. It is assumed that crack-tip transformation occurs when the remote stress intensity factor $K^{\infty}$ reaches a critical value and thus creates a crack-tip transformation zone extending a distance $r$ from the crack tip. The critical stress intensity factor $K_c$ depends on particle size, temperature, chemical composition, and material stiffness.

Consider plane strain crack problems under mode I loads in which the stress fields are symmetric with respect to the crack. The functions $f_{ij}(\theta)$ are universal and can be found in many textbooks. For the crack in the material considered here, the stresses and strains are unbounded at the crack tip. Therefore, the material near the crack tip is fully transformed. It is assumed that $K^{\text{tip}}$ governs the fracture processes at the tip and then the stress field becomes

$$\sigma_{ij} = \frac{K^{\text{tip}}}{\sqrt{2\pi r}} \cdot f_{ij}(\theta) \tag{5}$$

The reduction from $K^{\infty}$ to $K^{\text{tip}}$ determines the toughening effect due to the transformation.

The relationship between crack tip shielding and toughness change is established using the crack-advance mechanism. For brittle materials, crack growth generally occurs by direct advance of the crack tip and, hence, crack-tip stresses are of primary significance. However, the stresses ahead of the crack tip may be significant for SMAs since they exhibit a peculiar inelastic behavior. Near the tip region, the linearity of the stress–strain curve at large strains indicates that the near tip stress be characterized by the stress intensity factor $K^{\text{tip}}$. The crack-tip stress intensity factor is smaller than the stress intensity factor $K^{\infty}$ associated with the applied remote field. The reduced stress intensity $\Delta K$ can be defined as

$$\Delta K = K^{\infty} - K^{\text{tip}} \tag{6}$$

which corresponds directly to the change of fracture toughness. The crack propagates when $K^{\text{tip}}$ attains the toughness of the fully transformed material ahead of the crack tip $K_c$. The applied stress intensity at crack advance becomes

$$K_c^{\infty} = K_c^{\text{tip}} + \Delta K_c \tag{7}$$

The toughness change due to transformation can then be evaluated by $\Delta K_c$.

### 2.3. Shape and size of transformation zone

The boundary of the transformation can be determined approximately by the undisturbed remote stress field when the transformation strain is very small. However, if the transformation strain is not small, the remote stress field around the transformation zone will be disturbed by the crack tip stress field. Evans (1984) pointed out that the transformation zone determined by the remote stress field is bigger than that by the crack tip stress field. By following Evans (1984), the boundary of the transformation zone is approximately determined by the average value of $K^{\infty}$ and $K^{\text{tip}}$ and the stress intensity factor after transformation is defined as

$$K = \left(K^{\infty} + K^{\text{tip}}\right)/2 \tag{8}$$

For plane strain problems, only $\sigma_x$, $\sigma_y$, $\tau_{xy}$ exist. Under the mode I loading, the stresses induced by the remote stress intensity factor $K$ at a distance $r$ away from the crack tip are given by

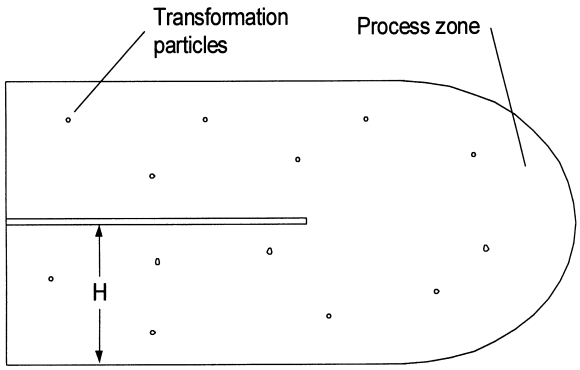


Fig. 2. The fully developed transformation zone with a semi-infinite wake.

$$\sigma_x = \frac{K}{\sqrt{2\pi r}}\cos\frac{\theta}{2}\left[1 - \sin\frac{\theta}{2}\sin\frac{3\theta}{2}\right]$$

$$\sigma_y = \frac{K}{\sqrt{2\pi r}}\cos\frac{\theta}{2}\left[1 + \sin\frac{\theta}{2}\sin\frac{3\theta}{2}\right]$$

$$\tau_{xy}\frac{K}{\sqrt{2\pi r}}\sin\frac{\theta}{2}\cos\frac{\theta}{2}\cos\frac{3\theta}{2} \tag{9}$$

The yield condition of shape memory alloys is defined as (Sun and Hwang, 1993a, 1993b; Fischer et al., 1996)

$$\frac{g}{\sqrt{3}}\sigma_e - \frac{1}{2}B_1(T)g^2\xi - C_0(T,\xi) = 0 \tag{10}$$

$$\sigma_e = \left(\frac{3}{2}S_{ij}S_{ij}\right)^{1/2}$$

$$S_{ij} = \sigma_{ij} - \sigma_m\delta_{ij}$$

$$\sigma_m = \frac{1}{3}\sigma_{ii} \tag{11}$$

By substituting the crack tip stress equations (9) into the yield condition (10), the transformation zone for static cracked shape memory alloys can be expressed as

$$\sqrt{r(\theta)} = \frac{1}{\sqrt{2\pi}}\cdot\left[\frac{K}{\sigma_e^c(T,\xi)}\right]\cdot\cos\frac{\theta}{2}\left(1 + 3\sin^2\frac{\theta}{2}\right)^{1/2} \tag{12}$$

with

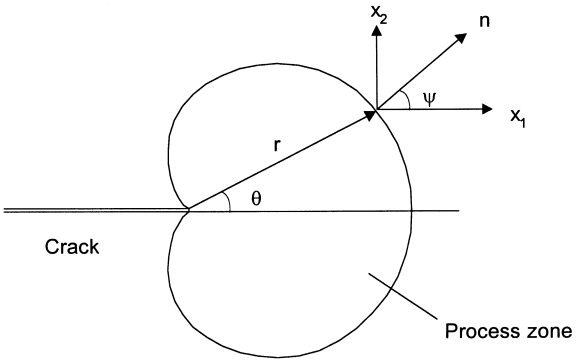


Fig. 3. Coordinate system used for the stress analysis.

$$\sigma_e^c(T,\xi) = \frac{\sqrt{3}}{g}\left[(a+b\xi)(T-M_s)\right] \tag{13}$$

where $M_s$ is the temperature of martensite start, $a$, $b$ are the material constants and $\sigma_e^c$ is a parameter which depends on temperature, chemical composition, and material moduli.

When the applied load exceeds the initial critical fracture toughness, crack growth will occur. With increasing the applied load, the crack will propagate stably until it is in the steady-advanced state. After that, the crack will propagate unstably. As the crack advances under steady-state conditions, transformation occurs along a curve ahead of the crack tip, and in the wake region behind, no further transformation occurs as shown in Fig. 2 (Budiansky et al., 1983; Evans, 1984). The crack growth is assumed to occur at a constant critical value of the crack-tip stress intensity factor $K_c$ and the shape of the transformation zone will change into a new shape with a long transformed wake. The half height of the wake $H$ is

$$H = \max\left\{r(\theta)\sin\theta\right\} \tag{14}$$

Combining Eqs. (12) with (14) leads to

$$H = \frac{1}{2\pi}\cdot\left[\frac{K}{\sigma_e^c(T,\xi)}\right]^2\cdot\cos^2\frac{\hat{\theta}}{2}\left(1+3\sin^2\frac{\hat{\theta}}{2}\right)\sin\hat{\theta} \tag{15}$$

where $\hat{\theta}\approx 82^\circ$.

When the crack advances at a constant $K$ into the initial transformation zone leaving behind a semi-infinite wake the half height of which is $H$ and reaches the steady-state, the boundary of the transformation zone for steady advanced cracked materials can be determined by Eq. (15) as

$$r(\theta) = \begin{cases} H\cdot\dfrac{\cos^2\dfrac{\theta}{2}\left[1+3\sin^2\dfrac{\theta}{2}\right]}{\cos^2\dfrac{\hat{\theta}}{2}\left[1+3\sin^2\dfrac{\hat{\theta}}{2}\right]\sin\hat{\theta}} & 0\le|\theta|\le\hat{\theta} \\ \dfrac{H}{\sin(\theta)} & \hat{\theta}\le|\theta|\le\pi \end{cases} \tag{16}$$

### 2.4. Derivation of transformation strains

As shown in Fig. 3, transformation particles can be treated as inclusions and inhomogeneities and then the following equation can be obtained using Eshelby's equivalent method (Eshelby, 1957)

$$C_{ijkl}\left(\epsilon^0_{kl} + \bar{V}_{klmn}\epsilon^{**}_{mn} - \epsilon^{**}_{kl}\right) = C^*_{ijkl}\left(\epsilon^0_{kl} + \bar{V}_{klmn}\epsilon^{**}_{mn} - \epsilon^p_{kl}\right) \tag{17}$$

with

$$\sigma^0_{ij} = C_{ijkl}\epsilon^0_{kl} \tag{18}$$

where $\epsilon^{**}_{kl}$ are uniform eigenstrains of the inclusion problem, $\epsilon^{\mathrm{p}}_{kl}$ are inelastic strains, $C_{ijkl}$ and $C^*_{ijkl}$ are the moduli of untransformed and transformed SMAs, respectively, $\sigma^0_{ij}$ and $\epsilon^0_{kl}$ are the applied remote stresses and corresponding strains, respectively, and Eshelby's variant matrix $\bar{V}_{klmn}$ is

$$\bar{V}_{ijkl} = \begin{bmatrix} \bar{V}_{1111} & \bar{V}_{1122} & \bar{V}_{1133} & 0 & 0 & 0 \\ \bar{V}_{2211} & \bar{V}_{2222} & \bar{V}_{2233} & 0 & 0 & 0 \\ \bar{V}_{3311} & \bar{V}_{3322} & \bar{V}_{3333} & 0 & 0 & 0 \\ 0 & 0 & 0 & \bar{V}_{1212} & 0 & 0 \\ 0 & 0 & 0 & 0 & \bar{V}_{2323} & 0 \\ 0 & 0 & 0 & 0 & 0 & \bar{V}_{3131} \end{bmatrix} \tag{19}$$

$$\bar{V}_{1111} = \bar{V}_{2222} = \frac{5-4\nu}{8(1-\nu)}$$

$$\bar{V}_{3333} = 0$$

$$\bar{V}_{1122} = \bar{V}_{2211} = \frac{1-4\nu}{8(1-\nu)}$$

$$\bar{V}_{3311} = \bar{V}_{3322} = 0$$

$$\bar{V}_{1133} = \bar{V}_{2233} = \frac{\nu}{2(1-\nu)}$$

$$\bar{V}_{1212} = \frac{3-4\nu}{8(1-\nu)}$$

$$\bar{V}_{1313} = \bar{V}_{2323} = \frac{1}{4} \tag{20}$$

Eq. (17) can be rewritten as

$$\left[C_{ijkl}\bar{V}_{klmn} - C^*_{ijkl}\bar{V}_{klmn} - C_{ijmn}\right]\epsilon^{**}_{mn} = C^*_{ijkl}\epsilon^0_{kl} - C_{ijkl}\epsilon^0_{kl} - C^*_{ijkl}\epsilon^p_{kl} \tag{21}$$

Hence, the transformation strain $\epsilon^t_{ij}$ and its time derivative $\dot{\epsilon}^t_{ij}$ can be obtained as

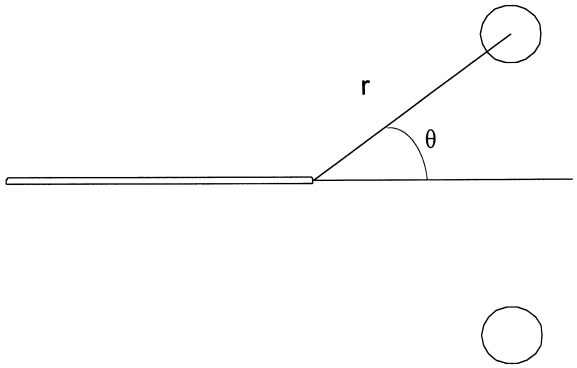


Fig. 4. Two symmetric circular transformation spots near a crack tip.

$$\epsilon_{ij}^{\mathrm{t}} = \epsilon_{ij}^{**} = \left[C_{ijkl}\bar{V}_{klmn} - C^{*}_{ijkl}\bar{V}_{klmn} - C_{ijmn}\right]^{-1}\left[C^{*}_{mnkl}\epsilon^{0}_{kl} - C_{mnkl}\epsilon^{0}_{kl} - C^{*}_{mnkl}\epsilon^{p}_{kl}\right]$$

$$= \left[C_{ijkl}\bar{V}_{klmn} - C^{*}_{ijkl}\bar{V}_{klmn} - C_{ijmn}\right]^{-1}\left[C^{*}_{mnkl}C^{-1}_{klgh}\sigma^{0}_{gh}\sigma^{0}_{mn} - C^{*}_{mnkl}\epsilon^{p}_{kl}\right] \tag{22}$$

$$\dot{\epsilon}_{ij}^{t} = \left[C_{ijkl}\bar{V}_{klmn} - C^{*}_{ijkl}\bar{V}_{klmn} - C_{ijmn}\right]^{-1}\left[C^{*}_{mnkl}C^{-1}_{klgh}\dot{\sigma}^{0}_{gh} - \dot{\sigma}^{0}_{mn} - C^{*}_{mnkl}\dot{\epsilon}^{\mathrm{p}}_{kl}\right]$$

The inelastic strains $\epsilon^{p}_{kl}$ can be determined from the constitutive relation. Substituting Eq. (1) into (23) yields the transformation strains induced by the inelastic strains of SMA inclusions.

### 2.5. Toughening effects of transformation

The stress intensity induced at a crack tip by the transformation of one particle can be calculated by Eshelby's method (Eshelby, 1957). It is assumed that the particle is removed from the matrix, and the particle undergoes the unconstrained transformation with the strain $\epsilon^{\mathrm{t}}$. The original shape of the particle can be restored by applying surface traction $\mathbf{Q}_{\mathrm{c}} = -\mathbf{n}\mathbf{C}\epsilon^{\mathrm{t}}$, where $\mathbf{C}$ is the moduli of the particle and $\mathbf{n}$ is the outward surface normal vector as shown in Fig. 3. The two symmetric particles fit into the unloaded matrix from which they were removed and the equilibrium can be established by nullifying the constraining surface traction with a layer of body forces.

The principle of linear superposition shows that the stress intensity factor due to the transformation that occurs in the unloaded body is the stress-intensity change imposed when the transformation occurs in a stressed specimen. The stress intensity factor due to the traction $\boldsymbol{Q} = -\mathbf{Q}_{\mathrm{c}} = \mathbf{n}\mathbf{C}\epsilon^{\mathrm{t}}$ applied to the particle periphery can be computed for inclusions of arbitrary shape and elasticity. However, the present study is restricted to the case of a long cylindrical particle as shown in Fig. 4 whose axis is parallel to the crack front. The material properties of the particle are different from those of the matrix. Thus, it is an inhomogeneity inclusion problem. The cylindrical particle represents either a large number of finite particles distributed through the specimen thickness or, in another application, the entire transformation zone.

Table 1
Material properties of shape memory alloys (Brinson and Lammering, 1993)

| $E_a$ (MPa) | $E_m$ (MPa) | $\Theta$ (MPa/K) | $\epsilon_L$ | $M_f$ (K) | $M_s$ (K) | $A_s$ (K) | $A_f$ (K) | $C_m$ (MPa/K) | $C_a$ (MPa/K) | $\sigma_s^{cr}$ (MPa) | $\sigma_f^{cr}$ (MPa) |
|---|---|---|---|---|---|---|---|---|---|---|---|
| $67 \times 10^3$ | $30 \times 10^3$ | 0.55 | 0.067 | 282 | 291 | 308 | 322 | 8 | 13.8 | 100 | 170 |

A useful tool for calculating the stress intensity factor due to the traction **Q** is the weight function proposed by Bueckner (1970). Then it was further elaborated by Paris et al. (1976). The weight functions **h** for plane strain deformation are shown as (McMeeking and Evans, 1982)

$$\boldsymbol{h} = \begin{Bmatrix} h_x \\ h_y \end{Bmatrix} = \frac{1}{2\sqrt{\pi}(1-\nu)\sqrt{r}} \cdot \begin{Bmatrix} \cos\frac{\theta}{2}\left(2\nu - 1 + \sin\frac{\theta}{2}\sin\frac{3}{2}\theta\right) \\ \sin\frac{\theta}{2}\left(2 - 2\nu - \cos\frac{\theta}{2}\cos\frac{3}{2}\theta\right) \end{Bmatrix} \tag{23}$$

which dominates the weight function near the crack tip only. For the remote field, nonsingular terms become significant, with the result that the weight-function values on the free surfaces of finite bodies differ significantly from Eq. (23). In most cases the region of transforming particles near the tip is within the area of dominance of Eq. (23). In addition, the stress induced by the transformation of cylindrical particles diminishes by the inverse square of the distance from the particle. This implies that typical surface traction required to nullify transformation-induced stresses at external surfaces is negligibly small. Consequently, the reduced stress intensity factor induced by the transformation of cylindrical particles near the crack tip can be computed from

$$\Delta K^{\text{tip}} = \frac{E}{1-\nu}\int_{S_p}\left[\mathbf{n}\epsilon^t\mathbf{h} + \frac{\nu}{1-2\nu}\epsilon^t\mathbf{n}\mathbf{h}\right] \mathrm{d}S_p \tag{24}$$

where $S_p$ is the perimeter of the particle. For the mode I loading, $\epsilon^t$ is symmetric. By using the Gaussian integral equation, Eq. (24) can be rewritten as

$$\Delta K^{\text{tip}} = \frac{E}{1-2\nu}\int_A \mathrm{div}(\epsilon^t \cdot \mathbf{h})\, \mathrm{d}A \tag{25}$$

where $A$ is the transformation area.

By combining Eqs. (23) and (25), the rate of the reduced crack tip stress intensity factor due to the transformation becomes

$$\Delta\dot{K} = \frac{E}{1-2\nu}\int_A \left(F_1\dot{K} + F_2\dot{T}\right) \mathrm{d}A \tag{26}$$

where $F_1$ and $F_2$ are the kernel functions which depend on the material characteristics and temperature.

## 3. Results and discussion

Firstly, transformation boundaries are calculated. The material properties of TiNi based SMAs used for this study are given in Table 1. The remote loading increases proportionally and monotonically.

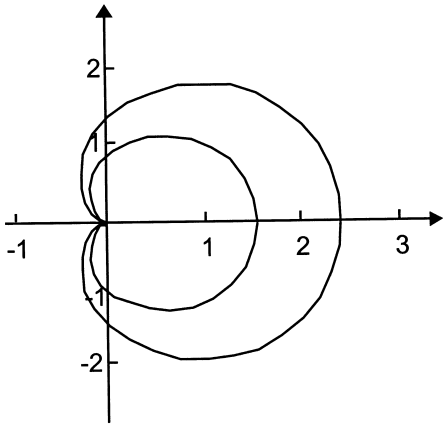


Fig. 5. The boundaries of transformation start and finish zones at $T = 38^{\circ}C$ for static cracks.

Then the material near the crack tip possesses a tripartite structure. In the inner most region, the maximum stress exceeds the transformation finish critical stress and the material is fully transformed. In the outer most region, the stresses are below the transformation threshold and the material is untransformed. Between these two zones, there is a transition region where the material is partially transformed. Fig. 5 illustrates the transformation starting and finishing boundaries at temperature $T = 38^{\circ}C$. The outer curve is the transformation start curve while the inner one is the transformation finish curve. Under the mode I loading, the symmetric configuration is obtained. It is seen that the shapes of the two curves are very similar except that the radii are different.

Secondly, the effect of applied loads on crack tip SIFs is studied. Fig. 6 illustrates the crack tip SIF versus the applied remote loading at the temperature $T = 38^{\circ}C$. The results show that the ratio between the crack tip SIF and the applied load is reduced when the applied loading increases beyond the critical stress. This is because the extent of the transformation increases when the applied remote stress increases continuously. As a result, the rate of the reduced crack tip SIF increases and the toughness of SMAs increases.

Thirdly, consider thermal and mechanical loads shown in Fig. 7. At first, the temperature is $38^{\circ}C$ and

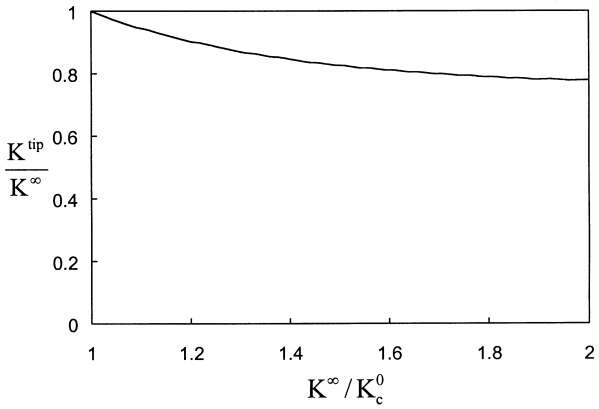


Fig. 6. The crack tip SIF with respect to the applied remote loading at $T = 38^{\circ}C$

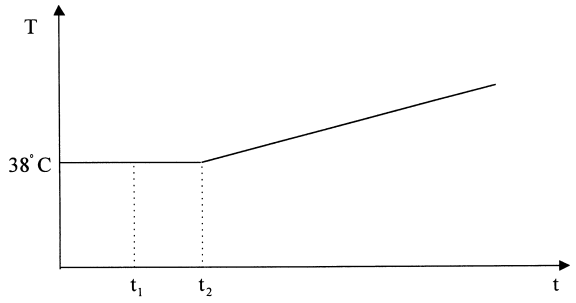


(a)

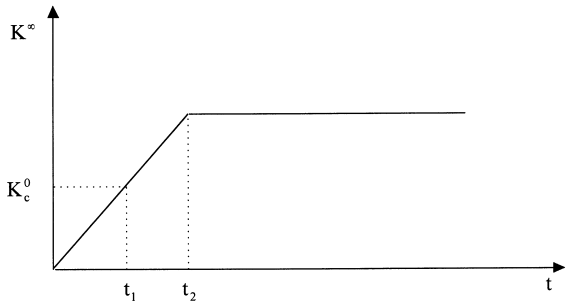


(b)

Fig. 7. Thermal and mechanical loads: (a) temperature curve; (b) applied loads.

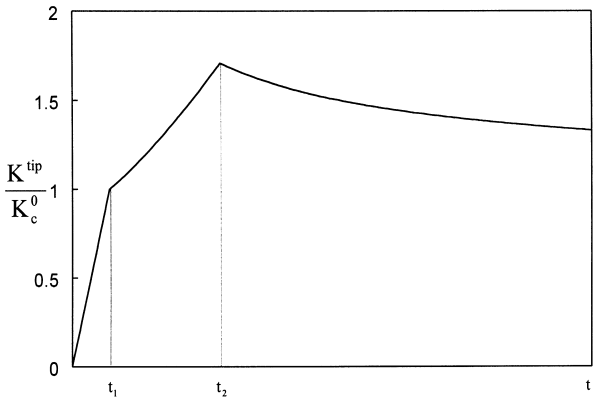


Fig. 8. The crack tip SIF.

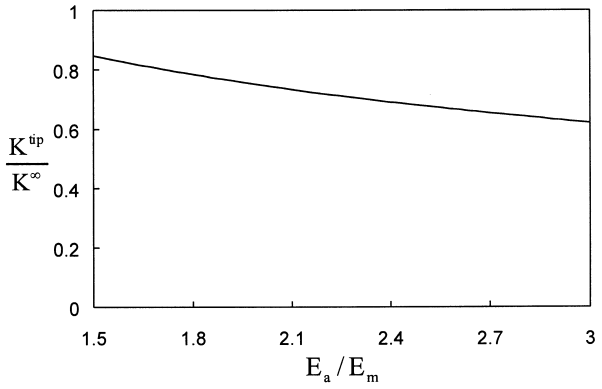


Fig. 9. The crack tip SIF versus modulus ratio at temperature $T = 38°C$.

the applied remote stress increases from zero to the transformation initial value $K_c^0$ at time $t_1$ and further to the value $K^\infty = 2.15K_0^c$, at time $t_2$ as shown in Fig. 7(b). Then the applied load remains constant, the temperature increases from 38 to 88°C as shown in Fig. 7(a). Fig. 8 shows the crack tip SIF during the loading process. During the time interval $0$–$t_1$, the load increases from 0 to $K_c^0$ and the crack growth does not occur during this period. The crack tip SIF increases linearly with increasing the remote load. When the load surpasses the $K_c^0$ during the time interval $t_1$–$t_2$, the transformation toughening results in the slow increase of crack tip SIFs as shown in Fig. 6. The crack tip is shielded during this period. After time $t_2$, the load remains constant and temperature increases. Then the crack tip SIF is greatly decreased with increasing temperature. This phenomenon shows that increasing temperature is a feasible way to release the crack tip SIF or relax the crack tip stress after crack growth has taken place.

Next the effects of the ratio between untransformed and transformed SMAs moduli $E_a/E_m$ on the toughness mechanism of SMAs are studied. The mechanical load is applied between the initial fracture toughness $K_c^0$ and final fracture toughness $K_c$ at isothermal conditions. Fig. 9 illustrates the relation between the normalized crack tip stress intensity factor (SIF) and the modulus ratio at $T = 38°C$. In general, the moduli of transformed SMAs are smaller than those of untransformed materials. It shows that the crack tip SIF decreases with increasing the modulus ratio. This study shows that the greater reduction of the crack tip stress intensity can be achieved by using larger modulus ratios.

Lastly steady-advanced cracks are considered. For steady-advanced crack problems, the crack is stable when the applied load is below the critical value of crack propagation and no crack propagation occurs when the applied loading does not increase. When the applied load is above the critical value of the crack propagation, the crack advances unstably even at a constant loading. The critical value of crack propagation is related to the fracture toughness $K_c$ which is a material characteristic constant and depends on temperature. It should also be noticed that the applied remote stress does not affect the value of $K_c$. Isothermal conditions are considered in this study. The analytic results show a significant toughening effect. The non-dimensional toughness $K_c/K_c^0 = 1.23$ is obtained at $T = 38°C$.

## 4. Conclusions

Shape memory alloys with semi-infinite cracks subjected to the mode I loading are considered. By using Eshelby's inclusion method and the weight function method, fracture toughness mechanism due to

martensite transformation mechanism is investigated. The shape and size of the transformation zones for both stationary and steady advanced cracks have been analyzed. The studies show that martensite transformation reduces the crack tip stress intensity and increases the toughness of SMAs. Temperature seems to play an important role in the toughening process of SMAs. The crack tip SIF is greatly decreased with increasing temperature. It is a feasible way to relax the crack tip stress after crack growth has taken place. The study also shows that the greater reduction of the crack tip stress intensity can be achieved by using the larger ratio between untransformed and transformed SMAs moduli.

## References


Achenbach, M., Muller, I., 1983. Creep and yield in martensitic transformation. Ingenieur-Archiv 1, 16–28.

Achenbach, M., Muller, I., 1986. A model for memory alloys in plastic strains. International Journal of Solids and Structures 22, 166–278.

Birman, V., 1997. Review of mechanics of shape memory alloy structures. Applied Mechanics Review 50, 629–645.

Boyd, J., 1994. Thermomechanical response of shape memory composites. Journal of Intelligent Material Systems and Structures 5, 455–473.

Brinson, L., Huang, M., 1996. Simplification and comparisons of shape memory alloy constitutive models. Journal of Intelligent Material Systems and Structures 7, 108–114.

Brinson, L., Lammering, R., 1993. Finite element analysis of the behavior of shape memory alloys and their applications. International Journal of Solids and Structures 30, 3261–3280.

Budiansky, B., Hutchinson, J., Lambropoulos, J., 1983. Continuum theory of dilatent transformation toughening in ceramics. International Journal of Solids and Structures 19, 337–355.

Bueckner, H., 1970. A novel principle for the computation of stress intensity factor. Mechanics of Materials 50, 529–533.

Chopra, I., 1996. Review of current status of smart structures and integrated systems. SPIE 2717, 20–62.

Eshelby, J., 1957. Determining of the elastic field of an ellipsoidal inclusion and related problem. Proceedings of Royal Society 241, 376–396.

Evans, A., 1984. Toughening mechanism in zirconia alloys. Advanced Ceramics 12, 193–212.

Fischer, F., Sun, Q., Tanaka, K., 1996. Transformation-induced plasticity (TRIP). Applied Mechanics Review 49, 317–364.

Funakubo, H., 1984. Shape Memory Alloy. Gordon and Breach, London.

Lagoudas, D., Moorthy, D., Qidwai, M., Reddy, J., 1997. Modelling of the thermomechanical response of active laminates with SMA strips using the laywise finite element method. Journal of Intelligent Material Systems and Structures 8, 476–488.

Liang, C., Rogers, C., 1990. One-dimensional thermomechanical constitutive relations for shape memory materials. AIAA Journal 901027, 16–28.

Liang, C., Rogers, C., 1991. The multi-dimensional constitutive relations for shape memory alloys. AIAA Journal 911165, 178–185.

McMeeking, R., Evans, A., 1982. Mechanics of transformation-toughening in brittle materials. Journal of American Ceramic Society 65, 242–246.

Paris, P., McMeeking, R., Tada, H., 1976. The weight function method for determining stress intensity factors. Crack and Fracture of ASTM-STP 601, 471–489.

Shen, L., Yu, S., 1996. Mechanics of dilatant transformation in one side of bimaterial interface. Engineering Fracture Mechanics 54, 239–248.

Stam, G., Giessen, E., 1995. Effect of reversible phase transformations on crack growth. Mechanics of Materials 21, 51–71.

Sun, Q., Hwang, K., 1993a. Micromechanics modelling for the constitutive behavior of polycrystalline shape memory alloys. Journal of Mechanical Physics and Solids 41, 1–19.

Sun, Q., Hwang, K., 1993b. Micromeehanics modelling for the constitutive behavior of polyerystalline shape memory alloys. Journal of Mechanical Physics and Solids 41, 20–33.

Tanaka, K., 1986. Thermomechanics of transformation pseudoelasticity and shape memory effect in alloys. International Journal of Plasticity 2, 59–72.

Tanaka, K., 1990. A phenomenological description on thermomechanical behavior of shape memory alloy. Journal of Pressure Vessel Technology 112, 158–163.